

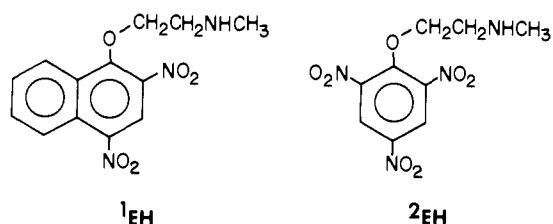
# Toward a Complete Characterization of the Mechanism of Nucleophilic Aromatic Substitution by an Amine. Kinetics of Spiro Meisenheimer Complexes Derived from *N*-Methylethanolamine<sup>1</sup>

Claude F. Bernasconi,\* Constantin L. Gehriger, and Rita H. de Rossi

Contribution from the Thimann Laboratories of the University of California, Santa Cruz, California 95064. Received June 1, 1976

**Abstract:** The kinetics of the reversible conversion of *N*-methyl- $\beta$ -aminoethyl 2,4-dinitronaphthyl ether hydrochloride ( $1_{EH_2^+}$ ) into *N*-methyl-*N*- $\beta$ -hydroxyethyl-2,4-dinitronaphthylamine ( $1_{AH}$ ), and of *N*-methyl- $\beta$ -aminoethyl picryl ether hydrochloride ( $2_{EH_2^+}$ ) into *N*-methyl-*N*- $\beta$ -hydroxyethyl picramide ( $2_{AH}$ ) has been studied in aqueous solution. The reaction occurs in two distinct stages, characterized by two relaxation times. The first is very rapid; it involves equilibrium deprotonation of  $EH_2^+$  (Scheme I) followed by intramolecular nucleophilic attack by the  $N-CH_3$  group to form a zwitterionic spiro Meisenheimer complex and deprotonation of the zwitterionic complex to form the more stable anionic form of the complex. The second stage is relatively slow and involves the conversion of the complex into the final product AH by three concurrent mechanisms: (a) C-O bond breaking in the anionic complex, followed by rapid protonation of the negative oxygen; (b) general acid catalyzed C-O bond breaking in the anionic complex which leads directly to AH, presumably by a concerted process; (c) direct conversion of the zwitterionic complex into AH for which four possible mechanisms are discussed. By simultaneously applying the temperature-jump, stopped-flow, the combined stopped-flow temperature-jump, and conventional kinetic techniques the rate constants for all the important elementary steps could be determined. Some of the most significant results and conclusions are (a) that in the first stage proton transfer between the zwitterionic and anionic forms of the complex is partially rate limiting, (b) that the  $pK_a$  values of the zwitterionic complexes are quite low ( $\sim 6$ ), (c) that the transition states in the formation of the five-membered spiro complexes always appear to be complex like, and (d) that general acid catalysis of C-O bond breaking is rather weak. The implications of this last point with respect to the mechanism of general base catalysis in nucleophilic aromatic substitution are discussed.

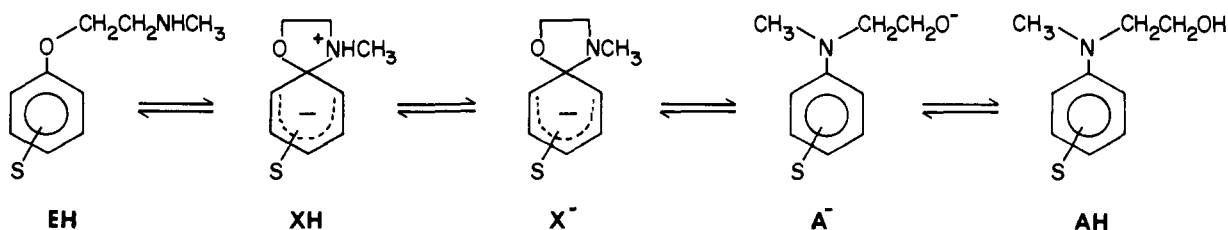
Scheme I constitutes an intramolecular nucleophilic aromatic substitution of an alkoxide ion by a secondary amine.<sup>2</sup> We found that the two substrates  $1_{EH}$  and  $2_{EH}$  are sufficiently



activated to permit a kinetic study of the various elementary steps involved. Apart from the challenge of characterizing all elementary steps of a complex reaction, knowledge of these rate constants has great value for the detailed understanding of the mechanism of nucleophilic aromatic substitution by amines.<sup>3</sup>

The system of Scheme I poses some experimental problems not previously encountered in simpler model systems.<sup>4</sup> They stem from a combination of two features. The first is that the equilibration of the process  $EH \rightleftharpoons XH \rightleftharpoons X^-$  is very rapid (typical relaxation times 20  $\mu$ s–2 ms) which necessitates the use of the temperature-jump (TJ) relaxation method. The second is that, at the pH values suitable for the study of the  $EH \rightleftharpoons XH \rightleftharpoons X^-$  process, AH is thermodynamically by far the most stable species of the entire system. Although the equi-

Scheme I

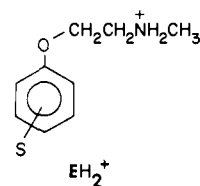


bration of the process  $X^- \rightleftharpoons A^- \rightleftharpoons AH$  is much slower than that of the process  $EH \rightleftharpoons XH \rightleftharpoons X^-$ , it is still fast enough, in the picryl derivative ( $2$ ), to convert essentially all of the substrate into the AH form in a few minutes or less, i.e., before a decent TJ experiment could be performed. Hence these experiments had to be carried out by the combined stopped-flow temperature-jump (SF-TJ) method.<sup>5</sup>

We now report a complete kinetic study for compounds  $1$  and  $2$  in aqueous solution at 25 °C.

## Results

**Mechanism and General Features.** A complete reaction scheme is shown in Scheme II. Note that it includes an additional species,  $EH_2^+$ , not shown in Scheme I, which is in rapid equilibrium with EH. The definitions of  $k_1$  and  $k_{-1}$  are ob-



vious;  $k_4^{OH}$  and  $k_{-4}^{OH}$  refer to the uncatalyzed transformation  $X^- \rightleftharpoons A^-$ ,  $k_4^B$  and  $k_{-4}^B$  to the presumably concerted general acid-base catalyzed reaction  $X^- + BH \rightleftharpoons AH + B^-$ ;  $k_2$  and  $k_{-2}$  represent the direct conversion  $XH \rightleftharpoons AH$  although not

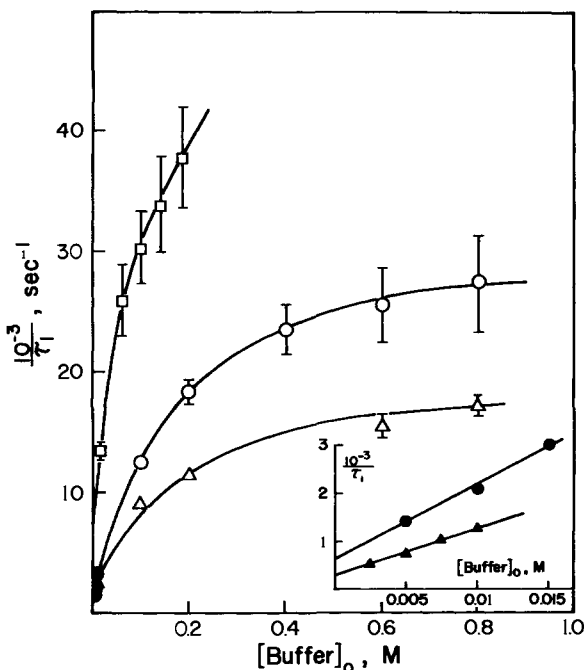
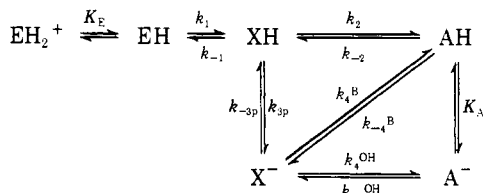


Figure 1. Representative plots of  $1/\tau_1$  vs. total buffer concentration for 1: (□) phosphate buffer, pH 7.40; (○) Tris buffer, pH 8.60; (●) Tris buffer, pH 8.64; (△) Tris buffer, pH 8.20; (▲) Tris buffer, pH 8.23.

#### Scheme II



necessarily by a concerted mechanism (see Discussion);  $k_{3p}$  and  $k_{-3p}$  (the subscript p stands for proton transfer) are defined by eq 1 and 2 where  $k_{3p}^{\text{S}}$ ,  $k_{3p}^{\text{OH}}$ , and  $k_{3p}^{\text{B}}$  refer to the deprotonation of XH by the solvent, by  $\text{OH}^-$ , and by a buffer base, respectively, while  $k_{-3p}^{\text{S}}$ ,  $k_{-3p}^{\text{OH}}$ , and  $k_{-3p}^{\text{B}}$  refer to the protonation of  $\text{X}^-$  by  $\text{H}^+$ , by the solvent, and by a buffer acid, respectively. Our analysis will permit evaluation of all mentioned rate constants as well as the acid dissociation constant of AH,  $k_A$ , can be estimated.

$$k_{3p} = k_{3p}^{\text{S}} + k_{3p}^{\text{OH}}[\text{OH}^-] + k_{3p}^{\text{B}}[\text{B}] \quad (1)$$

$$k_{-3p} = k_{-3p}^{\text{S}}[\text{H}^+] + k_{-3p}^{\text{OH}} + k_{-3p}^{\text{B}}[\text{BH}] \quad (2)$$

Kinetic determinations were carried out in aqueous buffers, at various pH values, always under pseudo-first-order conditions and at constant ionic strength of 0.5 M, maintained by addition of NaCl. Two relaxation effects, with the relaxation times  $\tau_1$  and  $\tau_2$ , respectively, were observed.  $\tau_1$  refers to the fast process and is associated with the equilibration of  $\text{EH}_2^+ \rightleftharpoons \text{EH} \rightleftharpoons \text{XH} \rightleftharpoons \text{X}^-$ , while  $\tau_2$  is the slow process, associated with the three reactions  $\text{XH} \rightleftharpoons \text{AH}$ ,  $\text{X}^- \rightleftharpoons \text{A}^- \rightleftharpoons \text{AH}$ , and  $\text{X}^- + \text{BH} \rightleftharpoons \text{AH} + \text{B}^-$ , but always with  $\text{EH}_2^+ \rightleftharpoons \text{EH} \rightleftharpoons \text{XH} \rightleftharpoons \text{X}^-$  acting as fast preequilibrium.

In order to study  $\tau_1$  by the TJ method two conditions have to be fulfilled. The first is that a substantial fraction of the total substrate concentration is present in the forms  $\text{EH}_2^+$ , EH, XH, and  $\text{X}^-$  (rather than AH and  $\text{A}^-$ ); this is necessary in order to assure concentration changes in at least one of these four species which are large enough for spectroscopic detection. For the case where the equilibrium strongly favors AH and  $\text{A}^-$  this cannot be achieved by compensating with a very high substrate concentration because of solubility limitations.

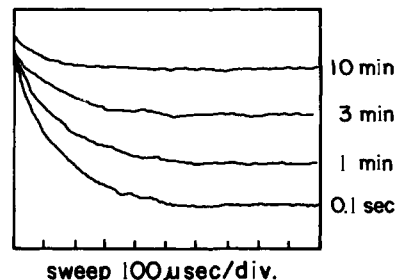


Figure 2. Typical oscilloscope traces in SF-TJ experiment for 2, in phosphate buffer (0.01 M), pH 6.93, as function of time elapsed after mixing.

The second condition is that the ratio  $([\text{XH}] + [\text{X}^-]) : ([\text{EH}_2^+] + [\text{EH}])$  be not too extreme, in order to assure a satisfactory relaxation amplitude.<sup>6</sup>

In a completely equilibrated solution these two conditions are not easily met at the same time. Thus in strongly acidic or strongly basic media the first but not the second condition can be met.<sup>7</sup> At intermediate pH values the second condition is easily fulfilled but not the first because AH becomes the dominant species.<sup>8</sup> The two conditions can, however, be met simultaneously by generating the four species  $\text{EH}_2^+$ , EH, XH, and  $\text{X}^-$  in situ by either of the following methods. One involves rapid (in the SF-TJ apparatus for 2) acidification of a strongly basic (pH > 12) solution of  $\text{X}^-$ , prepared either by dissolving the easily accessible AH form<sup>9</sup> in strong base or by dissolving the potassium salt of  $\text{X}^-$ <sup>9</sup> in strong base. The basis of this method is that  $\text{X}^-$ , upon acidification, first generates the kinetically controlled products XH, EH, and  $\text{EH}_2^+$  before the thermodynamically controlled AH has had time to form.<sup>10</sup> In the other method the pH of a strongly acidic solution of  $\text{EH}_2^+$  is raised rapidly. We have used both methods with identical results.

**First Relaxation Time.** The system  $\text{EH}_2^+ \rightleftharpoons \text{EH} \rightleftharpoons \text{XH} \rightleftharpoons \text{X}^-$  is completely analogous to Scheme I in ref 4b or eq 2 in ref 4a.<sup>11</sup> In fact, the reciprocal relaxation time,  $1/\tau_1$ , has the same qualitative dependence on pH and on buffer concentrations as in these earlier systems. Again in analogy to these earlier systems we can treat the reaction  $\text{EH}_2^+ \rightleftharpoons \text{EH}$  as rapid pre-equilibrium and XH as a steady-state intermediate which leads to

$$\frac{1}{\tau_1} = \frac{k_1 k_{3p}}{k_{-1} + k_{3p} K_E + [\text{H}^+]} + \frac{k_{-1} k_{-3p}}{k_{-1} + k_{3p}} \quad (3)$$

Note that in eq 3 as well as in subsequent equations  $[\text{H}^+]$  is defined as  $[\text{H}^+] = a_{\text{H}^+} / \gamma_{\text{H}^+}$ , where  $a_{\text{H}^+} = 10^{-\text{pH}}$ ,  $\gamma_{\text{H}^+} = 0.74$  is the trace activity coefficient in 0.5 M NaCl.<sup>12</sup>

For the naphthyl derivative (1)  $1/\tau_1$  was determined in a conventional TJ apparatus, as function of buffer concentration at a given pH. Several series, some at high buffer concentrations (typically 0.1 to 1.0 M), some at low concentrations (typically 0.005 to 0.015 M) were determined. Figure 1 shows a few representative plots whereas all experimental data, collected over a pH range from 6.7 to 8.85 (total of 63 data points), are summarized in Table I.<sup>13</sup>

For the picryl derivative (2) the experiments were done in the SF-TJ apparatus. Figure 2 shows a typical oscilloscope trace as a function of the time elapsed after mixing an acidic solution of  $\text{EH}_2^+$  with base. The relaxation amplitude is seen to have decreased by 50% after about 2 min, due to conversion into the AH form.

The use of the SF-TJ method made it difficult to adjust the pH of the reaction solutions to any predetermined value. Hence, instead of measuring  $1/\tau_1$  vs. buffer concentration at constant pH we measured  $1/\tau_1$  vs. pH at constant buffer concentration (for details see Experimental Section). Figures

Table III.  $1/\tau_1(\text{hi})$  and  $1/\tau_1(\text{no})$  for Picryl System (2)

pH	$1/\tau_1(\text{hi}), \text{s}^{-1}$		$1/\tau_1(\text{no}), \text{s}^{-1}$	
	Exptl	Calcd	Exptl	Calcd
6.20	33 200	32 800	12 400	13 300
6.40	24 600	24 000	8 800	8 470
6.60	18 200	17 000	5 800	5 490
6.80	13 500	12 150	4 400	3 700
7.00	10 200	9 110	3 600	2 710
7.20	9 000	8 040	2 600	2 250
7.40	8 400	8 430		
7.60	10 200	10 250	2 450	2 940
7.70	11 200	11 870	3 300	3 250

Table IV.  $1/\tau_1(\text{hi})$ ,  $k_{-1}/k_{3p}^B$ , and  $1/\tau_1(\text{no})$  for the Naphthyl System (1)

pH	$1/\tau_1(\text{hi}), \text{s}^{-1}$		$k_{-1}/k_{3p}^B, \text{M}$	$1/\tau_1(\text{no}), \text{s}^{-1}$	
	Exptl	Calcd		Exptl	Calcd
6.70				3240	3220
6.80				2840	2590
6.90				2000	2010
7.015				1640	1565
7.275				960	860
7.40	>50 000	68200	$0.054 \pm 0.018^a$		
7.56				580	466
7.78				340	382
8.01				240	346
8.20	$20\,000 \pm 6000$	19400	$0.21 \pm 0.08^b$		
8.23				260	386
8.44				400	416
8.60	$27\,000 \pm 8000$	21200	$0.12 \pm 0.06^b$		
8.64				600	555
8.85				980	1020

<sup>a</sup> Phosphate buffer. <sup>b</sup> Tris buffer.

3 and 4 show our data while Table II<sup>13</sup> contains all numerical results.

**$1/\tau_1$  at High Buffer Concentrations.** Plots of  $1/\tau_1$  vs. buffer concentration approach a plateau value at high concentration. In mechanistic terms this plateau corresponds to the condition  $k_{3p} \approx k_{3p}^B[B] \gg k_{-1}$ , i.e., deprotonation of XH becomes faster than the reversion of XH to EH. Here eq 3 simplifies to<sup>14</sup>

$$\frac{1}{\tau_1(\text{hi})} = k_1 \frac{K_E}{K_E + [H^+]} + k_{-1} \frac{[H^+]}{K_X} \quad (4)$$

where  $K_X$  is the acid dissociation constant of XH.

In the picryl system  $1/\tau_1(\text{hi})$ <sup>15a</sup> was obtained by drawing vertical lines through the pH profiles of Figures 3 and 4 and plotting the intersecting points vs. buffer concentration. Most of these plots virtually reached the plateau at high concentration and thus allowed one to obtain  $1/\tau_1(\text{hi})$  directly. They are summarized in the first column in Table III.

In the naphthyl system the plots of  $1/\tau_1$  vs. buffer concentration did not quite reach the plateau; they were treated as follows. Since, except at the very lowest buffer concentrations, the  $k_{3p}^B[B]$  and  $k_{-3p}^B[BH]$  terms of eq 1 and 2, respectively, are dominant, eq 3 becomes

$$\frac{1}{\tau_1} = \frac{k_1 k_{3p}^B[B]}{k_{-1} + k_{3p}^B[B]} \frac{K_E}{K_E + [H^+]} + \frac{k_{-1} k_{-3p}^B[BH]}{k_{-1} + k_{3p}^B[B]} \quad (5)$$

which, upon inversion and arithmetic manipulation, affords

$$\tau_1 = \tau_1(\text{hi}) + \tau_1(\text{hi}) \frac{k_{-1}(K_B + [H^+])}{k_{3p}^B K_B [B]_0} \quad (6)$$

where  $[B]_0$  is the total buffer concentration and  $K_B$  is the acid dissociation constant of the buffer acid. Thus a plot of  $\tau_1$  vs.  $[B]_0^{-1}$  affords  $\tau_1(\text{hi}) = \text{intercept}$ , whereas the slope permits one to find  $k_{-1}/k_{3p}^B$  according to the following equation:

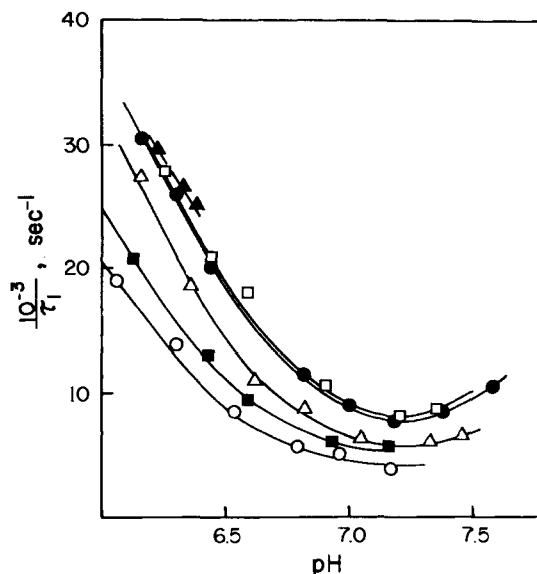


Figure 3.  $1/\tau_1$  vs. pH at various phosphate buffer concentrations for 2: (O) 0.005 M; (■) 0.01 M; (△) 0.02 M; (●) 0.1 M; (□) 0.2 M; (▲) 0.25 M.

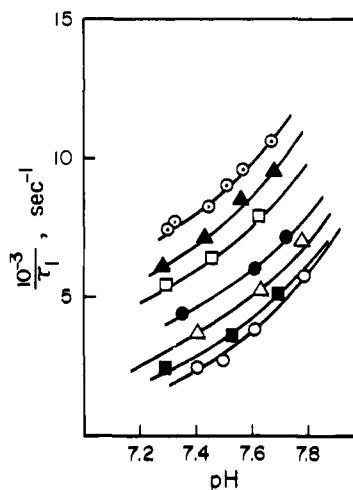


Figure 4.  $1/\tau_1$  vs. pH at various Tris buffer concentrations for 2: (O) 0.01 M; (■) 0.015 M; (△) 0.02 M; (●) 0.1 M; (□) 0.2 M; (▲) 0.3 M; (⊙) 0.5 M.

$$\frac{k_{-1}}{k_{3p}^B} = \frac{\text{slope}}{\tau_1(\text{hi})} \frac{K_B}{K_B + [H^+]} \quad (7)$$

The results of this analysis are summarized in the first and third columns of Table IV.

In the picryl system the  $1/\tau_1(\text{hi})$  data can be exploited to estimate  $k_{-1}/K_X$  as follows. We assume that, below pH 7, the  $k_1 K_E / (K_E + [H^+])$  term of eq 4 is negligible. Thus a plot of  $1/\tau_1(\text{hi})$  vs.  $[H^+]$  should be linear in that range, with a slope =  $k_{-1}/K_X$ . Such a plot (not shown) is in fact reasonably straight although it has a slight downward curvature at the highest hydronium ion concentrations. This curvature suggests that the implied assumption which underlies eq 4, viz. that  $K_X \gg [H^+]$ , starts to break down at the lowest pH values used and that eq 4 needs to be replaced by

$$\frac{1}{\tau_1(\text{hi})} = k_1 \frac{K_E}{K_E + [H^+]} + k_{-1} \frac{[H^+]}{K_X + [H^+]} \quad (8)$$

This will be borne out by the results of the spectrophotometric determination of  $K_X$  (see next section).

Hence we proceeded as follows. The initial slope of the plot of  $1/\tau_1(\text{hi})$  vs.  $[H^+]$  was used to estimate  $k_{-1}/K_X$  which

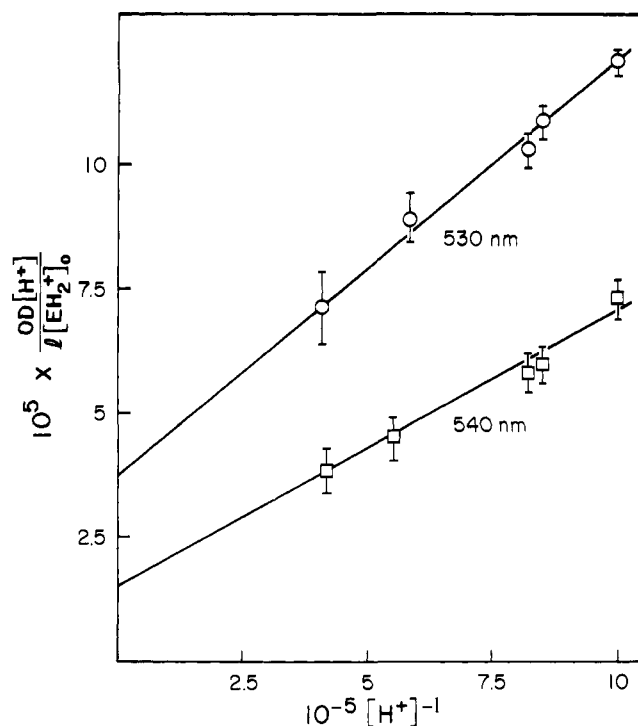


Figure 5. Spectrophotometric determination of  $K_X$  and  $K_E K_1$  for the picryl system, plot according to eq 8 at two different wavelengths;  $\epsilon_{530} = 8440$ ,  $\epsilon_{540} = 5670$ .

provided a good estimate of  $k_{-1}$  in conjunction with  $K_X$  determined spectrophotometrically. The value of  $k_{-1}$  was then later refined by a curve fitting procedure described in a subsequent section.

In the naphthyl system the high uncertainty in  $1/\tau_1(\text{hi})$  only permits a crude estimate of  $k_{-1}/K_X$  and thus of  $k_{-1}$ ; however, the results could be refined by the same curve fitting procedure as for the picryl system.

**Spectrophotometric Determination of  $K_X$  and  $K_E K_1$ .**  $K_X$  as well as  $K_E K_1$  ( $K_1 = k_1/k_{-1}$ ) were determined by the same spectrophotometric method used before.<sup>4</sup> A plot according to

$$\frac{\text{OD}[\text{H}^+]}{l[\text{EH}_2^+]_0} = \epsilon_{\text{XH}} K_E K_1 + \epsilon_{\text{X}^-} \frac{K_E K_1 K_X}{[\text{H}^+]} \quad (9)$$

where OD is the optical density,  $l$  is the path length, and  $[\text{EH}_2^+]_0$  is the stoichiometric substrate concentration, provides  $K_X$  as slope/intercept (assuming  $\epsilon_{\text{XH}} = \epsilon_{\text{X}^-}$ ) and  $K_E K_1$  as intercept/ $\epsilon_{\text{X}^-}$ ;  $\epsilon_{\text{X}^-}$  is known.<sup>9</sup> Two representative plots are shown in Figure 5. Our  $K_X$  and  $K_E K_1$  values represent the average from determinations at two or three different wavelengths. Due to rather low optical densities, particularly at the lowest pH values (typical OD range from 0.02 to 0.1), we estimate the error limit to be rather high. As a consequence there will be a considerable uncertainty in the parameters calculated on the basis of  $K_X$  or  $K_1 K_E$  (see below).

We can now use  $K_X$  in combination with  $k_{-1}/K_X$  determined from  $1/\tau_1(\text{hi})$  to obtain  $k_{-1}$ .

**$1/\tau_1$  at Low Buffer Concentration.** At low concentration  $1/\tau_1$  increases linearly with buffer concentration (see e.g., Figure 1). Both intercepts and slopes of such plots provide useful information. The intercepts are given by

$$\frac{1}{\tau_1(\text{no})} = \frac{k_1(k_{3p}^S + k_{3p}^{\text{OH}}[\text{OH}^-])}{k_{-1} + k_{3p}^S + k_{3p}^{\text{OH}}[\text{OH}^-]} \frac{K_E}{K_E + [\text{H}^+]} + \frac{k_{-1}(k_{-3p}^S[\text{H}^+] + k_{-3p}^{\text{OH}})}{k_{-1} + k_{3p}^S + k_{3p}^{\text{OH}}[\text{OH}^-]} \quad (10)$$

$1/\tau_1(\text{no})^{15b}$  values are summarized in Tables III and IV.

At low pH eq 10 greatly simplifies because the first term on the right hand side of the equation becomes negligible and  $k_{3p}^{\text{OH}}[\text{OH}^-] \ll k_{-1}$ . Furthermore, in the naphthyl system we have  $k_{-1} \gg k_{3p}^S$  so that for  $\text{pH} \leq 7.8$  eq 10 reduces to

$$1/\tau_1(\text{no}) = k_{-3p}^S[\text{H}^+] + k_{-3p}^{\text{OH}} \quad (11)$$

A plot of  $1/\tau_1(\text{no})$  vs.  $[\text{H}^+]$  (not shown) affords  $k_{-3p}^S$  as slope,  $k_{-3p}^{\text{OH}}$  as intercept. This then permits one to obtain  $k_{3p}^S = K_X k_{-3p}^S$  and  $k_{3p}^{\text{OH}} = K_X k_{-3p}^{\text{OH}}/K_w$  where  $K_w = 1.96 \times 10^{-14}$  is the ionic product constant of the solvent at ionic strength 0.5 M.

In the picryl system the first term on the right hand side of eq 10 only vanishes at  $\text{pH} \leq 6.6$ . Here we have  $k_{-3p}^S[\text{H}^+] \gg k_{-3p}^{\text{OH}}$ , but  $k_{3p}^S$  is not negligible compared with  $k_{-1}$ . Hence eq 10 becomes

$$\frac{1}{\tau_1(\text{no})} = \frac{k_{-1} k_{-3p}^S[\text{H}^+]}{k_{-1} + k_{3p}^S} \quad (12)$$

and a plot of  $1/\tau_1(\text{no})$  vs.  $[\text{H}^+]$  (not shown) affords  $k_{-1} k_{-3p}^S / (k_{-1} + k_{3p}^S)$  as slope. Substituting  $k_{3p}^S = K_X k_{-3p}^S$  in this slope leaves  $k_{-3p}^S$  as the only unknown which is thus determined.

This analysis does not provide  $k_{-3p}^{\text{OH}}$ . We estimate that  $k_{3p}^{\text{OH}}$  is about the same as that in the *N,N'*-dimethyl-*N*-picrylethylenediamine system<sup>4a</sup> ( $5.2 \times 10^9 \text{ M}^{-1} \text{ s}^{-1}$ ) and calculate  $k_{-3p}^{\text{OH}} = k_{3p}^{\text{OH}} K_w / K_X$ .

**Curve Fitting to Equations 4 (8) and 9.** At this stage all constants of eq 4 (8) and 9 except for  $k_1$  and  $K_E$  are known. These latter are now found by simultaneously fitting the pH dependence of both  $1/\tau_1(\text{hi})$  and  $1/\tau_1(\text{no})$  to eq 4 and 9, respectively, in the case of the naphthyl system, to eq 8 and 9, respectively, in the case of the picryl system. By also allowing  $k_{-1}$  to vary, the fit was considerably improved. The results of the best fit are shown in Tables III and IV. In view of the complexity of the system, we judge the fit as very satisfactory. The various kinetic and equilibrium parameters are summarized in Table V.

**Proton Transfer Rates (Buffers).** The initial slopes of the  $1/\tau_1$  vs.  $[\text{B}]_0$  plots (data at low buffer concentration) are given by

$$\text{initial slope} = \frac{k_1 k_{3p}^B \frac{K_E K_B}{(K_E + [\text{H}^+])(K_B + [\text{H}^+])} + k_{-1} k_{-3p}^B \frac{[\text{H}^+]}{K_B + [\text{H}^+]}}{k_{-1} + k_{3p}^S + k_{3p}^{\text{OH}}[\text{OH}^-]} \quad (13)$$

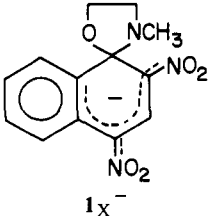
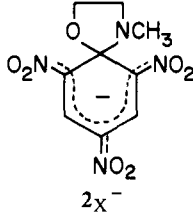
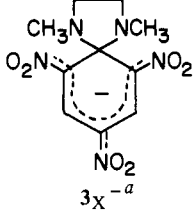
After substituting  $k_{-3p}^B$  with  $k_{3p}^B K_B / K_X$  we are left with  $k_{3p}^B$  as the only unknown in eq 13 from which it is calculated. The results, representing averages from slopes at several pH values are included in Table V. Note that the  $k_{-1}/k_{3p}^B$  ratios of Table IV agree, within experimental error, with those which can be calculated from  $k_{-1}$  and  $k_{3p}^B$  in Table V. This provides a test for internal consistency since the former is derived from data at high buffer concentration, the latter partially from data at low buffer concentration.

**Second Relaxation Time.** For the reciprocal second relaxation time which refers to the processes  $\text{XH} \rightleftharpoons \text{AH}$ ,  $\text{X}^- \rightleftharpoons \text{A}^- \rightleftharpoons \text{AH}$ , and  $\text{X}^- + \text{BH} \rightleftharpoons \text{AH} + \text{B}$ , coupled to the fast equilibrium  $\text{EH}_2^+ \rightleftharpoons \text{EH} \rightleftharpoons \text{XH} \rightleftharpoons \text{X}^-$ , one obtains

$$\frac{1}{\tau_2} = \frac{K_E K_1 k_2 [\text{H}^+] + K_E K_1 K_X (k_4^{\text{OH}} + k_4^{\text{B}} [\text{B}])}{K_E K_1 K_X + K_E (K_1 + 1) [\text{H}^+] + [\text{H}^+]^2} + \frac{k_{-2} [\text{H}^+] + K_A k_{-4}^{\text{OH}} + k_{-4}^{\text{B}} [\text{B}] [\text{H}^+]}{K_A + [\text{H}^+]} \quad (14)$$

$1/\tau_2$  was measured over a wide pH range and as function of

Table V. Summary of Results from First Relaxation Time and Spectrophotometric Determination of  $K_X$ 

			
	$1X^-$	$2X^-$	$3X^{-a}$
$K_E, M$ ( $pK_E$ )	$2.0 \pm 0.2 \times 10^{-9}$ (8.7)	$3.2 \pm 0.3 \times 10^{-9}$ (8.5)	$2.2 \times 10^{-9}$ (8.7)
$k_1, s^{-1}$	$4.6 \pm 2.7 \times 10^4$	$9.8 \pm 2.0 \times 10^4$	$1.20 \times 10^3$
$k_{-1}, s^{-1}$	$9.3 \pm 4.5 \times 10^6$	$1.2 \pm 0.3 \times 10^5$	$1.93 \times 10^5$
$K_1 = k_1/k_{-1}$	$4.9 \pm 3.0 \times 10^{-2}$	$8.2 \pm 4.0 \times 10^{-1}$	$6.2 \times 10^{-3}$
$K_X, M$ ( $pK_X$ )	$7.5 \pm 3.2 \times 10^{-7}$ ( $\approx 6.1$ )	$2.2 \pm 1.0 \times 10^{-6}$ ( $\approx 5.7$ )	$4.6 \times 10^{-7}$ ( $\approx 6.3$ ) <sup>b</sup>
$k_{3p}^S, s^{-1}$	$9.0 \pm 2.5 \times 10^3$	$4.3 \pm 1.2 \times 10^4$	$1.35 \times 10^4$
$k_{-3p}^S, M^{-1} s^{-1}$	$1.20 \pm 0.20 \times 10^{10}$	$2.10 \pm 0.40 \times 10^{10}$	$5.9 \times 10^{10}$
$k_{3p}^{OH}, M^{-1} s^{-1}$	$2.70 \pm 0.9 \times 10^9$	$5.2 \times 10^9$ <sup>c</sup>	$5.2 \times 10^9$
$k_{-3p}^{OH}, s^{-1}$	$7.0 \pm 1.4 \times 10^1$	$4.8 \times 10^1$	$4.45 \times 10^2$
$k_{3p}^{Phos}, M^{-1} s^{-1}$	$9.8 \pm 3.0 \times 10^6$	$8.0 \pm 3.0 \times 10^6$	$\approx 2 \times 10^7$
$k_{-3p}^{Phos}, M^{-1} s^{-1}$	$7.0 \pm 3.5 \times 10^6$	$1.9 \pm 0.7 \times 10^6$	$\approx 4.6 \times 10^7$
$pK_a^{Phos} - pK_X$ <sup>d</sup>	0.2	0.6	0
$k_{3p}^{Tris}, M^{-1} s^{-1}$	$8.0 \pm 3.0 \times 10^6$	$1.6 \pm 0.4 \times 10^7$	$\approx 10^7$
$k_{-3p}^{Tris}, M^{-1} s^{-1}$	$9.4 \pm 4.0 \times 10^4$	$6.4 \pm 2.0 \times 10^4$	$\approx 3.8 \times 10^5$
$pK_a^{Tris} - pK_X$ <sup>d</sup>	2.0	2.4	1.8

<sup>a</sup> Reference 4a. <sup>b</sup> Statistically corrected. <sup>c</sup> Assumed to be the same as for 3. <sup>d</sup>  $pK_a^{Phos} = 6.28$ ,  $pK_a^{Tris} = 8.06$  at 0.5 M ionic strength (ref 4a).

buffer concentration. Our data are summarized in Tables VI and VII.<sup>13</sup> Buffer dependence was weak or undetectable; thus under typical conditions, viz.  $[B]_0 \leq 0.05$  M, the  $k_4^B[BH]$  and  $k_{-4}^B[B][H^+]$  terms in eq 14 are negligible. The pH dependences of  $1/\tau_2$  are shown in Figure 6.

**$1/\tau_2$  at High pH.** At  $pH \geq 10.6$  we have  $K_E K_1 K_X \gg K_E (K_1 + 1)[H^+] + [H^+]^2$ ,  $k_2[H^+] \ll K_X k_4^{OH}$ , and  $k_{-2}[H^+] \ll K_A k_{-4}^{OH}$  in both systems so that eq 14 simplifies to

$$\frac{1}{\tau_2} = k_4^{OH} + k_{-4}^{OH} \frac{K_A}{K_A + [H^+]} \quad (15)$$

$1/\tau_2$  could conveniently be measured up to pH 12.8 for the picryl system, up to pH 13.5 in the naphthyl system; beyond that one quickly reaches the limit of the SF apparatus. As seen in Figure 6,  $\log 1/\tau_2$  depends linearly on the pH with a slope of one, indicating  $K_A \ll [H^+]$  up to the highest pH. Thus the slope of a plot of  $1/\tau_2$  vs.  $[H^+]^{-1}$  (not shown) is  $K_A k_{-4}^{OH}$  while the intercept is  $k_4^{OH}$ ;  $k_4^{OH}$  also corresponds to the plateau in the logarithmic plot of Figure 6.

**$1/\tau_2$  at Low pH.** At  $pH \leq 7.5$  for the naphthyl system, at  $pH \leq 6.5$  for the picryl system we have  $[H^+]^2 \gg K_E K_1 K_X + K_E (K_1 + 1)[H^+]$  so that, again neglecting buffer catalysis, eq 14 simplifies to

$$\frac{1}{\tau_2} = \frac{K_E K_1 k_2}{[H^+]} + \frac{K_E K_1 K_X k_4^{OH}}{[H^+]^2} + k_{-2} + \frac{K_A k_{-4}^{OH}}{[H^+]} \quad (16)$$

After rearranging one obtains

$$\left(\frac{1}{\tau_2} - k_{-2}\right)[H^+] = K_E K_1 k_2 + K_A k_{-4}^{OH} + \frac{K_E K_1 K_X k_4^{OH}}{[H^+]} \quad (17)$$

$k_{-2}$  is very small and was determined from initial rate measurements discussed in the next section.

In principle, a plot according to eq 17 would permit the evaluation of  $k_2$  because it is the only unknown in the intercept of such a plot. But the value so obtained would be very uncertain for two reasons. First, it is very sensitive to the errors in  $K_A k_{-4}^{OH}$  and  $K_E K_1$ . Second and more importantly, at the lowest pH values ( $pH \leq 6.3$  for the naphthyl,  $pH \leq 5.5$  for the

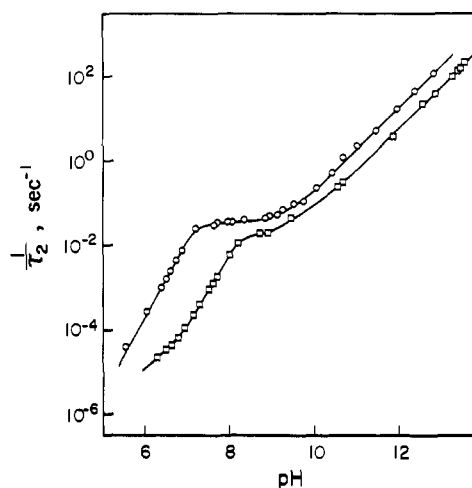


Figure 6. pH dependence of  $1/\tau_2$ ; data at low buffer concentration where buffer dependence is negligible: ( $\square$ ) naphthyl system (1); ( $\circ$ ) picryl system (2).

picryl system) which are necessary in order to obtain reasonably large intercepts, an unidentified decomposition reaction, presumably acid-catalyzed hydrolysis of EH and  $EH_2^+$ , started to compete and interfere with the  $\tau_2$  process, making  $\tau_2$  determinations unreliable in this range.

On the other hand, the slopes of plots according to eq 17, which are less sensitive to the above decomposition reaction, provide another way to evaluate  $k_4^{OH}$ . The agreement between this  $k_4^{OH}$  and the one determined directly according to eq 15 was well within experimental error; this provides another check of internal consistency with respect to  $K_1 K_E K_X$ .

**Method of Initial Rates.** Since the AH form does not appear to be subject to the decomposition reaction observed for the EH and  $EH_2^+$  forms, the determination of initial rates of the conversion of AH into  $EH_2^+$  permits more accurate measurements. We monitored the decrease in the concentration of AH in freshly prepared solutions of AH which were acidified to the desired pH in a acetic acid/acetate buffer. The data

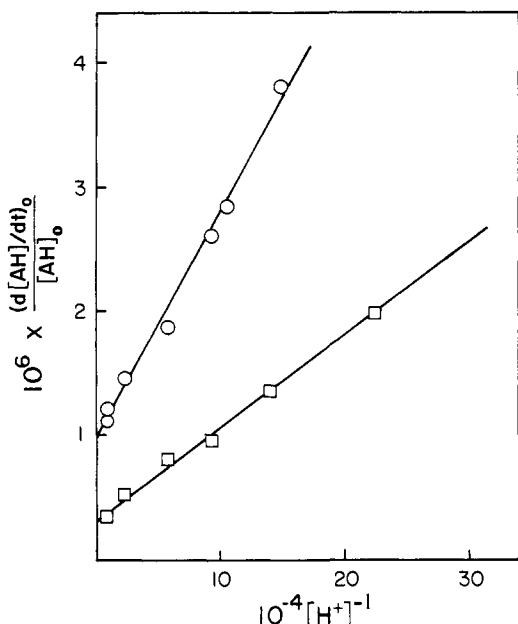


Figure 7. Initial rates as functions of  $[H^+]^{-1}$ , measured in an acetic acid/acetate buffer of  $[BH]_0 = 0.20$  M: ( $\square$ ) naphthyl system (1); ( $\circ$ ) picryl system (2).

which are summarized in Table VIII<sup>13</sup> were evaluated according to

$$\frac{(d[AH]/dt)_0}{[AH]_0} = k_{-2} + \frac{K_A k_{-4}^{OH}}{[H^+]} + k_{-4}^B \frac{K_B}{K_B + [H^+]} [BH]_0 \quad (18)$$

where  $(d[AH]/dt)_0/[AH]_0$  is equivalent to the initial slope of the absorbance vs. time curve, divided by the initial absorbance.<sup>17</sup> At low buffer concentrations ( $[BH]_0 \leq 0.02$  M) the buffer term in eq 18 is again negligible; plots of  $(d[AH]/dt)_0/[AH]_0$  vs.  $[H^+]^{-1}$  thus afford  $k_{-2}$  as intercept and  $K_A k_{-4}^{OH}$  as slopes (Figure 7). The latter agreed with  $K_A k_{-4}^{OH}$  determined from  $1/\tau_2$  at high pH within experimental error. From  $k_{-2}$  one now also obtains  $k_2 = k_{-2}/K_{-2}$  with  $K_{-2} = K_A K_{-4}^{OH}/K_X$ .

**Buffer Catalysis.** Buffer catalysis by acetic acid was detected at high concentrations by the method of initial rates. Plots of  $(d[AH]/dt)_0/[AH]_0$  vs.  $[BH]_0$  at constant pH are shown in Figure 8. According to eq 18 the slope is  $k_{-4}^B K_B / (K_B + [H^+])$  from which we obtain  $k_{-4}^B$  and finally  $k_4^B = k_{-4}^B K_B / K_A K_{-4}^{OH}$ .

## Discussion

The "grand prize" for the mechanistic chemist is to be able to characterize a complex reaction mechanism in as much detail as possible. Ideally this not only involves an elucidation of the structures of all intermediates and reasonable approximations of the transition states involved, but a complete mapping out of the free-energy profile of the reaction, i.e., a determination of the rate constants of all elementary steps. We believe we have come quite close to this ideal in this study. Our results are summarized in Table V and IX; some literature data which permit the evaluation of structural effects on some of the elementary processes of Scheme II are also included.

Before discussing the various rate or equilibrium constants, we should point out that in some cases the error limits are substantial, due to the propagation of errors in a complex mathematical analysis and/or due to the experimental difficulty of obtaining very good data in certain ranges. However, this should not distract from the principal conclusions, because

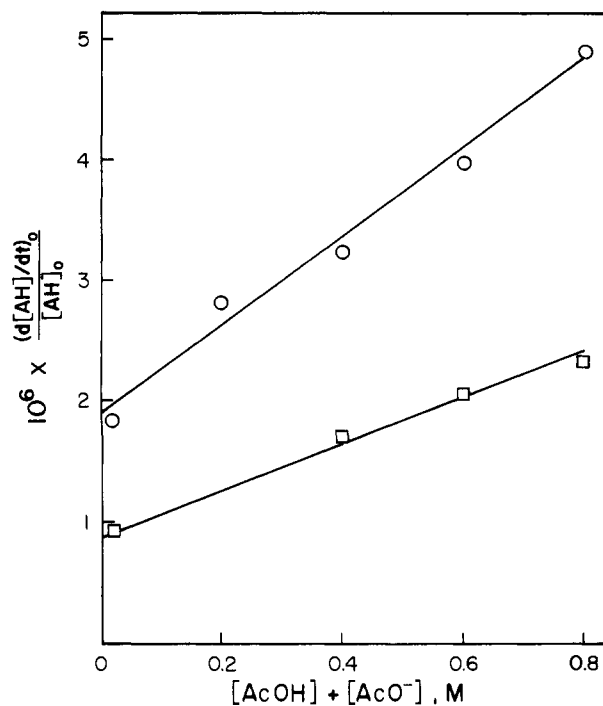


Figure 8. Initial rates as function of acetic acid/acetate buffer concentration: ( $\square$ ) naphthyl system (1), pH 5.10; ( $\circ$ ) picryl system (2), pH 4.89.

these will depend on effects much larger than the most conservatively estimated error limits.

**Rate-Limiting Proton Transfer.** Despite the fact that the deprotonation of XH by  $OH^-$  is virtually diffusion controlled<sup>18</sup> ( $k_{3p}^{OH} = 3-5 \times 10^9$  M<sup>-1</sup> s<sup>-1</sup>), the proton transfer between XH and  $X^-$  is partially rate limiting in the sequence  $EH \rightleftharpoons XH \rightleftharpoons X^-$ . This is a consequence of the high  $k_{-1}$  values which make  $k_{-1} \gg k_{3p}$  at low pH and low buffer concentrations. Thus the situation is quite analogous to that for **3**<sup>4a</sup> (see Table V); in fact for **2**  $k_{-1}$  is virtually the same as for **3**, whereas for **1**  $k_{-1}$  is about eightfold larger than for **2**, quite a reasonable result in view of the somewhat weaker activation in **1**.<sup>19</sup>

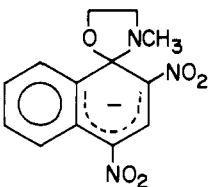
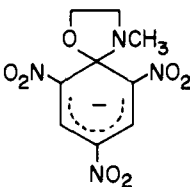
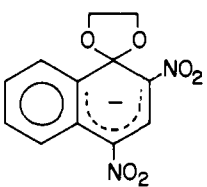
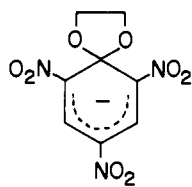
The implications of such high  $k_{-1}$  values with respect to the mechanism of base catalysis of nucleophilic aromatic substitution have been discussed elsewhere.<sup>4</sup>

**Proton-Transfer Rate Constants.** The value obtained for the rate constants (Table V) referring to the various proton-transfer pathways of the reaction  $XH \rightleftharpoons X^-$  are comparable with those found for system **3**.<sup>4a</sup> They conform to what one would expect on the basis of Eigen's<sup>18</sup> work. The first expectation is that the reactions  $X^- + H_3O^+ \rightarrow XH + H_2O$  ( $k_{-3p}^S$ ) and  $XH + OH^- \rightarrow X^- + H_2O$  ( $k_{3p}^{OH}$ ) are diffusion controlled or nearly so, while the rate constants of the respective reverse processes are determined by  $K_X$  and the respective forward rate constants. Secondly, one expects somewhat lower rates for proton transfers involving the buffer components, due to relatively small pK differences ( $pK_B - pK_X$ ) and furthermore due to steric hindrance (tris) or special features which are known to slow down proton transfer (borate). For a more detailed discussion of these effects see our earlier paper.<sup>4a</sup>

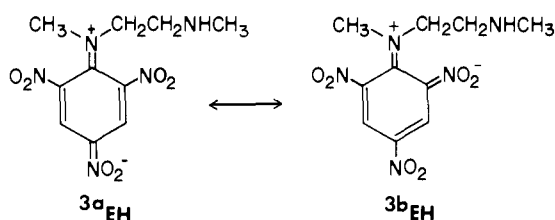
$k_1, k_{-1}, K_1$ . For **2**  $k_1$  is about twice as large as for **1**,  $k_{-1}$  about eight times smaller and  $K_1$  about 17 times larger (Table V). This is consistent with the somewhat higher activation in the picryl system.<sup>19</sup>

More interestingly,  $k_1$  and  $K_1$  for **2** are about 81- and 132-fold larger than for **3**, despite the fact that the basicity ( $K_E$ ) of the attacking  $HN-CH_3$  moiety is about the same in both systems. Possible factors accounting for the lower  $K_1$  in the case of **3** include greater ground-state resonance stabilization

Table IX. Summary of Results from Second Relaxation Time and Initial Rate Measurements

				
	1X-	2X-	4a	5a
$k_2, s^{-1}$	$1.0 \pm 0.5 \times 10^{-3}$	$2.8 \pm 1.5 \times 10^{-3}$		
$k_{-2}, s^{-1}$	$3.2 \pm 0.2 \times 10^{-7}$	$9.5 \pm 1.0 \times 10^{-7}$		
$K_{-2} = k_{-2}/k_2$	$3.2 \pm 1.7 \times 10^{-4}$	$3.4 \pm 1.7 \times 10^{-4}$		
$k_4^{OH}, s^{-1}$	$3.4 \pm 0.7 \times 10^{-2}$	$3.5 \pm 1.0 \times 10^{-2}$	2.3 <sup>b</sup>	$9.5 \times 10^{-2b}$
$K_A k_{-4}^{OH}, M^{-1} s^{-1}$	$8.3 \pm 1.0 \times 10^{-12}$	$2.6 \pm 0.2 \times 10^{-11}$	$1.8 \times 10^{-9c}$	$3.2 \times 10^{-8c}$
$K_A K_{-4}^{OH} = K_A k_{-4}^{OH}/k_4^{OH}, M^{-1}$	$2.4 \pm 0.7 \times 10^{-10}$	$7.4 \pm 1.5 \times 10^{-10}$	$6 \times 10^{-10b,c}$	$3.6 \times 10^{-7b,c}$
$k_4^{AcO}, M^{-1} s^{-1}$	$1.46 \pm 0.21 \times 10^{-1}$	$2.94 \pm 0.60 \times 10^{-1}$	25 <sup>b</sup>	0.9 <sup>b</sup>
$k_{-4}^{AcO}, M^{-1} s^{-1}$	$2.92 \pm 0.29 \times 10^{-6}$	$7.7 \pm 0.8 \times 10^{-6}$		
$k_4^S, M^{-1} s^{-1}$	$1.3 \times 10^3d$	$1.3 \times 10^3d$	$1.8 \times 10^4b,d$	$2.2 \times 10^3b,d$

<sup>a</sup> Reference 20. <sup>b</sup> Not statistically corrected. <sup>c</sup> Calculated from Crampton's<sup>29</sup> data by multiplication with  $K_W = 2 \times 10^{-14}$ . <sup>d</sup> See Discussion.



in the EH form of **3** (**3a**, **3b**), compared with **2**, and perhaps a larger steric strain (eclipsing effects) in the five-membered ring of the XH form of **3** compared with the XH form of **2**. Based on previous work<sup>20</sup> we believe the former effect to be the more important one.

It is noteworthy that in comparing **2** and **3** virtually the entire effect on  $K_1$  has its origin in a larger  $k_1$ , whereas  $k_{-1}$  is affected very little by the structural change. This suggests a transition state which is very much complex (XH)-like.

**$K_E$  and  $K_X$ .** Rather than emphasizing the slight differences in  $K_E$  (Table V) for **1**, **2**, and **3**,<sup>21</sup> we note that  $K_E$  is essentially the same for the three systems and about tenfold higher than the acid dissociation constant of the ammonio proton of  $HO-CH_2CH_2NH_3^+$ .<sup>22</sup> This indicates a strong electron-withdrawing effect of the picryl and 2,4-dinitronaphthyl moieties; resonance structures such as **3a**, **3b** may be partially responsible for this effect.

The  $K_X$  values show that XH is still substantially more acidic than  $EH_2^+$ . The inductive effect of the oxygen atom (of  $N-CH_3$  for **3**) can account for part of the effect but it appears that the picryl and the 2,4-dinitronaphthyl moieties add a substantial contribution to this electron-withdrawing effect, despite the negative charge.<sup>24</sup> This is in agreement with the findings of Crampton,<sup>25</sup> of Buncl and Webb,<sup>26</sup> and with theoretical calculations of Zollinger et al.<sup>27</sup> The  $K_X$  values reflect the expected greater electron-withdrawing effect of the picryl over the 2,4-dinitronaphthyl moiety (**2** vs. **1**) as well as the stronger inductive effect of oxygen compared with nitrogen (**2** vs. **3**).

**$K_A k_{-4}^{OH}$ ,  $k_4^{OH}$ ,  $K_A K_{-4}^{OH}$ .** The stability of  $X^-$  relative to AH ( $K_A K_{-4}^{OH}$ ) is about threefold higher for **2** compared with **1** (Table IX). Assuming that  $K_A$ <sup>28</sup> is about the same for both systems, this result would reflect a higher  $K_{-4}^{OH}$  for the more activated picryl system, as expected. Here it appears that the complex formation rate ( $K_A k_{-4}^{OH}$ ) is entirely responsible for the effect on  $K_A K_{-4}^{OH}$  while the decomposition rate ( $k_4^{OH}$ ) is about the same for both **1** and **2**; we recall that for the structural effect on  $K_1$  the main factor was a change in the rate of complex decomposition ( $k_{-1}$ ). This contrast is interesting

but too subtle to warrant an extensive discussion of the possible reasons at this time.

A comparison of **1** with **4**,<sup>29</sup> and of **2** with **5**<sup>29</sup> (Table IX) is interesting and more revealing. Let us first focus on the picryl systems **2** and **5**. Replacing the  $N-CH_3$  group by oxygen enhances  $K_A K_{-4}^{OH}$  about 500-fold. Since  $K_A$  is unlikely to be much different in the two systems, the main factor must be a greater  $K_{-4}^{OH}$  for **5**. Note that this is similar to the aforementioned enhancement of  $K_1$  when comparing **2** with **3** (Table V) and suggests a similar interpretation, viz. greater ground-state resonance stabilization in the  $A^-$  form of **2** compared with the  $A^-$  form of **5**, possibly coupled with a larger steric strain (eclipsing effects) in the five-membered ring of **2** compared with that of **5**; a third, additional factor may be a stabilizing effect of the two alkoxy substituents on the  $sp^3$  carbon of  $X^-$  for **5**.<sup>30</sup> A similar situation has been encountered before in comparing the stability constants ( $K_A K_{-4}^{OH}$ ) of the 2,4-dinitrophenyl analogous of **2** and **5** and was interpreted along the same lines.<sup>20</sup>

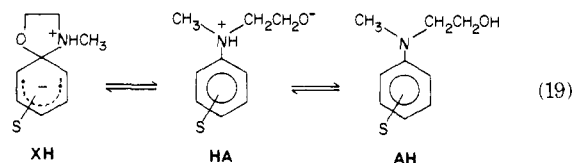
The enhancement of  $K_A K_{-4}^{OH}$  when changing from **2** to **5** is almost entirely due to an enhancement in the rate of complex formation ( $K_A k_{-4}^{OH}$ ), whereas the rates of complex decomposition ( $k_4^{OH}$ ) differ very little. This is similar to the situation with the 2,4-dinitrophenyl analogous of **2** and **5**<sup>20</sup> and also to the  $K_1$  process when comparing **2** with **3** discussed under the heading  $k_1$ ,  $k_{-1}$ ,  $K_1$ . It again suggests a complex ( $X^-$ )-like transition state.

Let us now compare **1** with **4**. Here the  $K_A K_{-4}^{OH}$  in the ethylene glycol derivative (**4**) is only 2.5 times higher than in the  $N$ -methylethanolamine derivative (**1**) but the complex **4** forms ( $K_A k_{-4}^{OH}$ ) about 200 times more rapidly than **1** while it also dissociates ( $k_4^{OH}$ ) about 70 times more rapidly. In view of the comparisons in the picryl series (this work) and the 2,4-dinitrophenyl<sup>20</sup> series, the situation in the naphthyl series appears rather "abnormal". We suggest that it is mainly **4** which behaves unexpectedly. This is best appreciated by comparing **4** with **5**. This comparison shows that  $K_A K_{-4}^{OH}$  is 600-fold smaller for **4** compared with **5**; such a large difference in complex stability between a picryl and a 2,4-dinitronaphthyl system is, to our knowledge, without precedent,<sup>19</sup> and we have currently no explanation for it.

**$k_2$ ,  $k_{-2}$ ,  $K_2$ .** The question of the mechanism of the conversion  $XH \rightleftharpoons AH$  is an interesting one, both with reference to the spiro complexes as well as in the context of the uncatalyzed pathway of nucleophilic aromatic substitutions by amines.<sup>3</sup>

There are four possible mechanisms, three of which are stepwise, one is a concerted process.

1. C-O bond breaking/formation and proton transfer be-

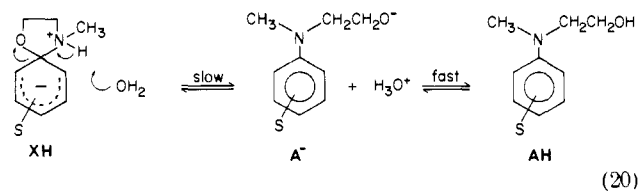


tween N and O occurs in separate steps, as shown in eq 19. Note that HA would be a very high energy intermediate. Let us consider two extremes.

a. The reaction  $HA \rightarrow XH$  is faster than reaction  $HA \rightarrow AH$  which makes the proton transfer  $AH \rightarrow HA$  the rate-determining step for the reverse reaction ( $k_{-2}$ ). This is not an attractive mechanism for the following reasons. Assuming a  $pK_a$  of HA of  $\sim -4.5$ <sup>31</sup> coupled with an estimated  $K_A \sim 3 \times 10^{-15}$ <sup>28</sup> leads to  $K = [HA]/[AH] \sim 10^{-19}$ . Thus in order to account for the experimental  $k_{-2}$  values (Table IX), the rate constant for the reaction  $HA \rightarrow AH$  would have to be  $> 3 \times 10^{12} \text{ s}^{-1}$ , a value considerably higher than that for typical intramolecular proton transfers.<sup>32</sup> Furthermore, such a high rate constant is contrary to the original assumption, viz. that the reaction  $HA \rightarrow AH$  should be slower than reaction  $HA \rightarrow XH$ .

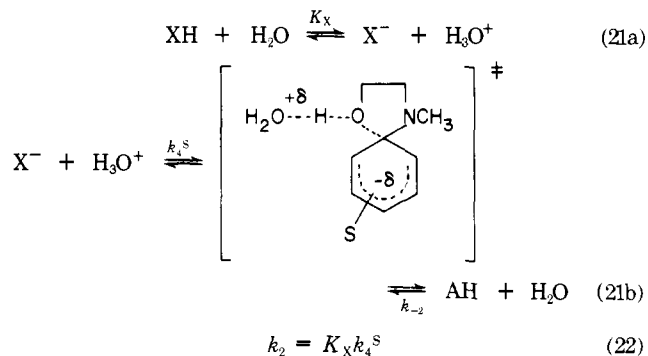
b. The reaction  $HA \rightarrow XH$  is slower than the reaction  $HA \rightarrow AH$  which makes C-O bond breaking the rate-determining step in the forward direction ( $k_2$ ). This mechanism can also be excluded by considering the implications for  $k_{-2}$ . Here  $k_{-2}$  is equal to  $K = [HA]/[AH]$  multiplied by the rate constant of the reaction  $HA \rightarrow XH$ . In order to account for the experimental  $k_{-2}$  values, it is now the reaction  $HA \rightarrow XH$  which would have to have a rate constant  $> 3 \times 10^{12} \text{ s}^{-1}$ , again too high to be realistic and again in contradiction to the original assumption that the reaction  $HA \rightarrow XH$  should be slower than the reaction  $HA \rightarrow AH$ .

2. Slow C-O bond breaking/formation concerted with proton transfer involving the solvent/hydronium ion in the first step, rapid protonation/deprotonation of the oxygen atom in the second step, as shown in eq 20.



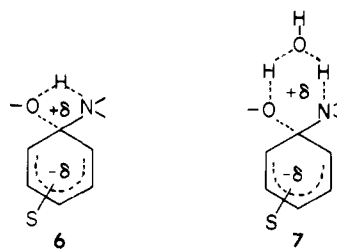
This mechanism is a reasonable possibility and provides a natural explanation as to why  $k_2$  is lower than  $k_4^{\text{OH}}$  (34-fold for **1**, 12.5-fold for **2**): in  $X^-$  ( $k_4^{\text{OH}}$  processes) the lone pair on the nitrogen atom is fully available to assist leaving group expulsion, whereas in the mechanism of eq 20 the lone pair is only partially available. This interpretation, though attractive, does not constitute a proof of this mechanism.

3. Fast proton transfer between  $XH$  and  $X^-$  in the first step, rate-limiting C-O bond breaking/formation catalyzed by the hydronium ion/solvent in the second step, as shown in eq 21. In this mechanism  $k_2$  is given by eq 22.



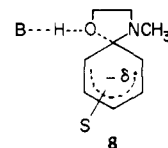
The equivalent of this mechanism was ruled out for the uncatalyzed pathway of nucleophilic aromatic substitutions by amines involving 2,4-dinitrophenyl or similarly activated substrates on the grounds that it requires unrealistically high  $k_4^S$  values (eq 22).<sup>33</sup> In the present situation, however, it is a perfectly reasonable mechanism. Indeed, the  $k_4^S$  values calculated on the basis of eq 21 (included in Table IX) are of comparable magnitude to the directly measurable rate constants of the hydronium ion catalyzed C-O bond breaking of the spiro complexes **4** and **5**. Whether this is a coincidence or should be taken as supporting evidence for this mechanism cannot be decided at present.

4. A mechanism which appeared to us as the most attractive possibility for the uncatalyzed pathway of nucleophilic aromatic substitutions by amines<sup>3</sup> is a concerted, intramolecularly acid catalyzed leaving group departure with a transition state such as **6** or **7**.



However, in spiro complexes the steric interference by the two methylene groups of the five-membered ring probably renders this mechanism impossible.

**General Acid/Base Catalysis,  $k_4^B$ ,  $k_{-4}^B$ .** We found that in an acetic acid/acetate buffer a general acid/base catalyzed pathway contributes to the reaction. This implies a mechanism which is probably concerted, with a transition state such as **8**.



We note that the relative importance of the catalytic pathway compared with that of the noncatalytic route, as measured by the ratios  $k_4^{\text{AcO}}/k_4^{\text{OH}}$ , is quite similar to that found in the respective ethylene glycol analogues **4** and **5** ( $k_4^{\text{AcO}}/k_4^{\text{OH}} = 4.3$  for **1**, 8.3 for **2**, 10.9 for **4**, 9.5 for **5**).

We feel that the significance of our results lies less in the fact that general catalysis is observed than in the smallness of the effect. Indeed it takes a  $\sim 1 \text{ M}$  concentration of acetic acid to achieve a mere fourfold acceleration of the conversion  $X^- \rightarrow AH$  in the case of **1**, or a  $\sim 0.5 \text{ M}$  concentration for the same acceleration in the case of **2**; with the less acidic general acids such as  $\text{HPO}_4^{2-}$ ,  $\text{trisH}^+$ ,  $\text{HCO}_3^-$ , or boric acid the catalytic effect was undetectable. These findings are significant in the context of the mechanism of general base catalysis in nucleophilic aromatic substitutions by amines.<sup>3</sup> The mechanism which has been most generally accepted is the SB-GA mechanism;<sup>3,34</sup> it involves a rapid equilibrium deprotonation of the initially formed zwitterionic intermediate complex (equivalent to  $XH$ ), followed by rate-limiting, general acid catalyzed leaving group expulsion (equivalent to  $k_4^B$  step in Scheme II).

Our results suggest that acid catalysis of leaving group departure by the acids present under typical reaction conditions of nucleophilic aromatic substitutions by amines, viz. the protonated amine nucleophile, is too weak to be significant. This then constitutes a further argument against the SB-GA mechanism as a general proposition, at least in protic media.<sup>35</sup>



## Experimental Section

**Materials.** *N*-Methyl-*N*- $\beta$ -hydroxyethyl-2,4-dinitronaphthylamine (**1**<sub>AH</sub>), *N*-methyl-*N*- $\beta$ -hydroxyethyl picramide (**2**<sub>AH</sub>), *N*-methyl- $\beta$ -aminoethyl 2,4-dinitronaphthyl ether hydrochloride (**1**<sub>EH<sub>2</sub><sup>+</sup></sub>), *N*-methyl- $\beta$ -aminoethyl picryl ether hydrochloride (**2**<sub>EH<sub>2</sub><sup>+</sup></sub>), and the respective spiro Meisenheimer complexes **1**<sub>X<sup>-</sup></sub> and **2**<sub>X<sup>-</sup></sub> were available from a previous study.<sup>9</sup> The buffers, HCl, NaOH, and NaCl were analytical grade commercial products and were used without further purification.

For solubility reasons it was sometimes more convenient to work with stock solutions of the substrate in Me<sub>2</sub>SO. After appropriate dilution the reaction solutions never contained more than 2% of Me<sub>2</sub>SO.

**Rate and Equilibrium Measurements.** For **1** the first relaxation time was measured on a Messanlagen<sup>36</sup> Transient Spectrophotometer. Typically, solutions equilibrated at 22 °C, were subjected to 3 °C temperature jumps, giving a reaction temperature of 25 °C. The relaxation effect was monitored at or near the absorption maximum of the X<sup>-</sup> form, viz. 500 to 530 nm.<sup>9</sup> The reaction solutions were usually prepared from acidic stock solutions of the EH<sub>2</sub><sup>+</sup> form to which the appropriate amount of buffer and electrolyte was added and whose pH was adjusted to the desired value as measured on a Corning digital pH meter. In some experiments the reaction solution was prepared starting with a stock solution of the X<sup>-</sup> form, or a stock solution of the AH form which was first made strongly basic (to generate X<sup>-</sup>) before adjusting it to the desired pH. The relaxation time was always found to be independent of the procedure used.

In the case of **2** the temperature-jump experiments were carried out on a Durrum<sup>37</sup> Model D-150 SF-TJ apparatus. In a typical experiment an unbuffered, slightly acidic solution of the EH<sub>2</sub><sup>+</sup> form (0.5 M ionic strength) was placed into one syringe of the SF-TJ apparatus, a buffered solution (0.5 M ionic strength) of approximately the desired pH into the other. The syringes were thermostated at 18 °C. The TJ pulse of 7 °C was triggered a few seconds after the two reagent solutions had been mixed, bringing the reaction solution to 25 °C. The pH of the reaction mixture was determined in a mock reaction solution, prepared by mixing, at 25 °C, two equal volumes of the stock solutions which had been used to fill the syringes of the SF-TJ apparatus. The relaxation effect was monitored between 427 and 520 nm ( $\lambda_{\text{max}}$  of X<sup>-</sup> 427 nm). An alternative procedure which was occasionally used was to replace the acidic EH<sub>2</sub><sup>+</sup> solution with an alkaline solution of the X<sup>-</sup> form in the first syringe. As with **1**, the relaxation time was independent of the procedure.

For both systems, the reported relaxation times represent the average of at least three independent oscilloscope traces.

In basic media (pH > 8.70 for **1**, pH  $\geq$  7.64 for **2**), the second relaxation time was determined on a Durrum<sup>37</sup> stopped-flow apparatus. At pH > 9.5, where the X<sup>-</sup> form is thermodynamically favored over the AH form, the process was initiated by mixing the AH form with base or an appropriate buffer while the relaxation process was monitored by recording the increase in absorption around 500 nm due to the formation of X<sup>-</sup>. At pH < 9.5 where AH is more stable than X<sup>-</sup> an inverse procedure was used, viz. the reaction was initiated by mixing the X<sup>-</sup> form with an appropriate acidic buffer and again monitored around 500 nm (decrease in absorption).

At pH  $\leq$  8.20 for **1**, pH  $\leq$  6.81 for **2** the second relaxation time was determined in a conventional (Gilford) kinetic spectrophotometer. Here the reaction was initiated by mixing an acidic solution of EH<sub>2</sub><sup>+</sup> with the appropriate buffer. Conversion of EH<sub>2</sub><sup>+</sup> into AH was monitored around 400 nm where the AH forms strongly absorb while absorption by EH<sub>2</sub><sup>+</sup> is minimal.<sup>9</sup>

The initial rate determinations were also carried out on the Gilford instrument. Here the decrease in absorption at 420 nm for **1**, at 390 nm for **2**, due to the conversion of AH into EH<sub>2</sub><sup>+</sup> was recorded after mixing an AH solution with the appropriate acidic buffer.

In the equilibrium ( $K_X$ ,  $K_E K_1$ ) determinations, the same general procedure described earlier<sup>4</sup> was used. However, due to the slow conversion into AH, several absorbance readings had to be taken at short time intervals immediately after preparing the solution; the absorption at zero time was then found by extrapolation.

**Acknowledgments.** This work was supported by grants from the National Science Foundation and the Alfred P. Sloan Foundation. A Frederick Gardner Cottrell equipment grant from the Research Corporation for the purchase of the tem-

perature-jump accessory to the Durrum stopped-flow apparatus is also gratefully acknowledged.

**Supplementary Material Available:** Tables I, II, VI, VII, and VIII summarizing all relaxation times and initial rate data (14 pages). Ordering information is given on any current masthead page.

## References and Notes

- (1) This is part 16 in the series "Intermediates in Nucleophilic Aromatic Substitution". Part 15: C. F. Bernasconi and H.-C. Wang, *J. Am. Chem. Soc.*, **98**, 6265 (1976).
- (2) Such intramolecular substitutions are also known as Smiles rearrangements, see e.g., (a) L. A. Warren and S. Smiles, *J. Chem. Soc.*, 956 (1930); (b) W. J. Evans and S. Smiles, *ibid.*, 181 (1935); (c) W. E. Truce, E. M. Kreider, and W. W. Brand, *Org. React.*, **18**, 99 (1970).
- (3) For a recent review dealing mainly with reactions of amines see C. F. Bernasconi, *MTP Int. Rev. Sci.: Org. Chem., Ser. One*, **1973**, 3, 33 (1973).
- (4) (a) C. F. Bernasconi and C. L. Gehringer, *J. Am. Chem. Soc.*, **96**, 1092 (1974); (b) C. F. Bernasconi and F. Terrier, *ibid.*, **97**, 7458 (1975).
- (5) (a) G. G. Hammes in G. G. Hammes "Techniques of Chemistry", Vol. VI, Part 2, Wiley-Interscience, New York, N.Y., 1974, p. 147; (b) C. F. Bernasconi, "Relaxation Kinetics", Academic Press, New York, N.Y., 1976, Chapter 11.
- (6) C. F. Bernasconi, "Relaxation Kinetics", Academic Press, New York, N.Y., 1976, Chapter 6.
- (7) For example, in the picryl system (**2**), [EH<sub>2</sub><sup>+</sup>] + [EH] + [XH] + [X<sup>-</sup>] amounts to >10% of the total substrate concentration at pH  $\leq$  6 but >99% is in the EH<sub>2</sub><sup>+</sup> form. At pH  $\geq$  11 [X<sup>-</sup>] amounts to >99% of the total substrate concentration.
- (8) For example, in the picryl system (**2**) we have ([XH] + [X<sup>-</sup>]):([EH<sub>2</sub><sup>+</sup>] + [EH])  $\approx$  1:10 at pH 6.6,  $\approx$  1:1 at pH 7.1,  $\approx$  10:1 at pH 7.6, but [EH<sub>2</sub><sup>+</sup>] + [EH] + [XH] + [X<sup>-</sup>] amounts to only  $\approx$  5% of the total substrate concentration at pH 6.6, to  $\approx$  0.5% at pH 7.6.
- (9) C. F. Bernasconi, R. H. de Rossi, and C. L. Gehringer, *J. Org. Chem.*, **38**, 2838 (1973).
- (10) This method was also used in making the EH<sub>2</sub><sup>+</sup> form on a preparative scale.<sup>9</sup>
- (11) Note that the symbols AH<sub>2</sub><sup>+</sup> and AH used previously<sup>4</sup> correspond to EH<sub>2</sub><sup>+</sup> and EH, respectively, in the present work.
- (12) H. S. Harned and R. A. Robinson in "Multicomponent Electrolyte Solution", Pergamon Press, Long Island City, N.Y., 1968, p. 50.
- (13) See paragraph concerning supplementary material at the end of this paper.
- (14)  $k_{3p} \approx k_{3p}^B [B]$  implies also  $k_{-3p} \approx k_{-3p}^B [BH]$ . Hence  $k_{-1} k_{-3p} / (k_{-1} + k_{3p})$  becomes (for  $k_{3p}^B [B] \gg k_{-1}$ )  $k_{-1} k_{-3p}^B [BH] / k_{3p}^B [B]$  which is equivalent to  $k_{-1} [H^+] / K_X$ .
- (15) (a) "hi" stands for high buffer concentration; (b) "no" stands for no buffer, or zero buffer concentration.
- (16) H. S. Harned and B. B. Owen, "The Physical Chemistry of Electrolytic Solutions", Reinhold, New York, N.Y., 1950, p. 486.
- (17) At a wavelength where AH is the only absorbing species. For details see Experimental Section.
- (18) M. Eigen, *Angew. Chem., Int. Ed. Engl.*, **3**, 1 (1964).
- (19) For recent reviews of Meisenheimer complexes, see (a) M. R. Crampton, *Adv. Phys. Org. Chem.*, **7**, 211 (1969); (b) M. J. Strauss, *Chem. Rev.*, **70**, 667 (1970).
- (20) C. F. Bernasconi and H. S. Cross, *J. Org. Chem.*, **39**, 1054 (1974).
- (21) The fact that  $K_E$  is somewhat larger for **2** compared with **1** and **3** is consistent with the expected stronger electron-withdrawing effect of the picryl compared with the 2,4-dinitronaphthyl moiety (2 vs. 1) and with the stronger inductive effect of oxygen compared with nitrogen (2 vs. 3).
- (22) The  $pK_a$  of H<sub>3</sub><sup>+</sup>NCH<sub>2</sub>CH<sub>2</sub>OH is 9.5.<sup>23</sup>
- (23) V. Sivertz, R. E. Reitmeyer, and H. V. Tartar, *J. Am. Chem. Soc.*, **62**, 1379 (1940).
- (24) Zwitterionic Meisenheimer complexes formed by attack of amines on 1,3,5-trinitrobenzene are also much more acidic than the conjugate acid of the attacking amine, despite the absence of an electron-withdrawing oxygen atom; see C. F. Bernasconi, M. Muller, and P. Schmid, in preparation.
- (25) M. R. Crampton, *J. Chem. Soc. B*, 2112 (1971).
- (26) E. Buncel and J. G. K. Webb, *Can. J. Chem.*, **52**, 630 (1974).
- (27) P. Caveng, P. B. Fisher, E. Heilbronner, A. L. Miller, and H. Zollinger, *Helv. Chim. Acta*, **50**, 848 (1967).
- (28)  $K_A$  is estimated to be  $2-5 \times 10^{-15}$  based on data of P. Ballinger and F. A. Long, *J. Am. Chem. Soc.*, **82**, 795 (1960).
- (29) M. R. Crampton and M. F. Willison, *J. Chem. Soc., Perkin Trans. 2*, 1681, 1686 (1974).
- (30) J. Hine, L. G. Mahone, and C. L. Liotta, *J. Am. Chem. Soc.*, **89**, 5911 (1967).
- (31) The  $pK_a$  of the conjugate acid of *N,N*-dimethyl picramide is  $\sim$ 4.8, L. P. Hammett and M. A. Paul, *J. Am. Chem. Soc.*, **56**, 827 (1934).
- (32) See e.g., (a) G. Maass and F. Peters, *Angew. Chem., Int. Ed. Engl.*, **11**, 428 (1972); (b) Z. Luz and S. Meiboom, *J. Am. Chem. Soc.*, **85**, 3923 (1963); (c) H. Diebler and R. N. F. Thorneley, *ibid.*, **95**, 896 (1973).
- (33) (a) C. F. Bernasconi and R. H. de Rossi, *J. Org. Chem.*, **38**, 500 (1973); (b) C. F. Bernasconi, R. H. de Rossi, and P. Schmid, in preparation.
- (34) M. R. Crampton in "Organic Reaction Mechanisms. 1973", A. R. Butler and M. J. Perkins, Ed., Wiley-Interscience, New York, N.Y., 1975, p. 225.
- (35) Other arguments were presented in ref. 4. In a forthcoming paper<sup>33b</sup> the problem of the mechanism of base catalysis in nucleophilic aromatic substitution will be discussed in its entirety.
- (36) Messanlagen Studiengesellschaft, Göttingen, Germany.
- (37) Durrum Instrument Corp., Palo Alto, Calif.